Proceedings of the Twenty-seventh (2017) International Ocean and Polar Engineering Conference **www.isope.org**
San Francisco, CA, USA, June 25-30, 2017

ISBN 978-1-880653-97-5; ISSN 1098-6189

Drag Coefficient Enhancement of Dual Cylinders in Oscillatory Flow

Dixia Fan[1], Xiaotong Zhang[2], Michael S. Triantafyllou[1]*
1 Department of Mechanical Engineering, Massachusetts Institute of Technology, Cambridge, MA, USA
2 State Key Laboratory of Ocean Engineering, School of Naval Architecture, Ocean and Civil Engineering, Shanghai Jiao Tong University, Shanghai, China

ABSTRACT

In this study, both experiments and numerical simulations have been performed to study sinusoidal oscillations of an identical pair of circular cylinders in a side-by-side configuration for various gaps in the still fluid. The key parameter of Keulegan-Carpenter (KC) number in the experiment is chosen between 0.5 and 20, Strokes number (β=Re/KC) values are selected from 350 to 2810 and gap ratio is selected from 0.5 to 3 in the experiments. Compared to the single cylinder cases, a large drag coefficient increase has been observed for gap ratios from 0.5 to 1.0. This phenomenon has later been confirmed by numerical simulations (in a smaller fixed Reynolds number of 120) using Lily-Pad, a solver built on boundary data immersed method (BDIM). In the numerical results, wake visualization shows that vortices shed from the cylinder pair will induce a jet between the gap, forming a vortex pair and accelerating the fluid particles away. This jet motion helps to expel energy from the structure into the fluid, and is confirmed by the energy flux calculation on the control volume around the cylinder pair, thus explains the enhancement of the drag coefficient.

KEY WORDS: dual cylinders; oscillatory flow; drag coefficient.

INTRODUCTION

Compared to the fluid structure interaction problem of cylinders open to the uniform flow that has been widely investigated, cylinders in the oscillatory flow has attracted less attention (Xu, 2013). However its significance cannot be undermined for its rich physics as well as its prevailing existence in all kinds of engineering scenario, especially in the ocean engineering field. As Fan (2016) pointed out that examples can be found in the offshore field such as the wave induced oscillatory flow around the risers, mooring lines, point wave energy generators, pump towers in the LNG ship experiencing sloshing load in the liquid tank induced by ship motion and blow-out preventers (BOP) forced to vibrate under the influence of upper riser motion, etc. In all these scenarios, the hydrodynamic model of the problems can be sufficiently simplified as fluid structure interaction in the oscillatory flow.

Under such conditions, the hydrodynamic inline forces on the structure can be expressed in Morison equation, which is proposed by Morison, Johnson and Schaaf (1950), as:

$$F = \frac{1}{2}\rho D C_d |U| U + \frac{1}{4}\pi\rho D^2 C_m \frac{dU}{dt} \qquad (1)$$

Where ρ, D, U are the fluid density, cylinder diameter, and relative velocity between cylinder and flow. C_d and C_m are the drag coefficient and added mass coefficient, which rely mainly on two non-dimensional parameters, the Keulegan-Carpenter (KC) number and Stokes β number. The KC number is defined as $KC = U_m T/D$, where U_m, T are the maximum vibrational velocity and oscillation period, and it can be simplified as $KC = 2\pi A/D$ for pure sinusoidal motion. And the Stokes β number is defined as $\beta = D^2/T\upsilon$, where υ is the kinematic viscosity of the fluid, and β can be interpreted as Re/KC, where Reynolds number $Re = U_m D/\upsilon$.

Bearman, et al. (1985) experimentally measured and reported the total force on a circular cylinder with various KC range of 4-55 and β from 100 to 1665, where they showed a good theory prediction on the drag coefficient for small KC range of $KC < 2$, while in the higher KC range, drag coefficient is found to be directly proportional to the KC number. Sarpkaya (1986) experimentally confirmed that the drag and added mass coefficient match with the theory under the critical KC number at which flow transits into unstable and depends on the different β number for the smooth cylinders. Apart from the force measurement, the flow visualization work performed by Williamson (1985) revealed the KC effect on the number of the vortex formation, where single pair to four pairs of vortex shedding is reported depending on the KC value. Later Tatsuno & Bearman (1990) carried out experiment for KC from 1.6 to 15 and β from 5 to 160，and they identified 8 different flow regimes (A^*, A, B, C, D, E, F, G).

Meanwhile, numerical works have been carried out on this problem to simulate the oscillatory flow past the circular cylinder. Uzunoglu, et al. (2001) modified the cell boundary element method to study oscillating cylinders in the still water, and detailed characteristics of experimental measurements of drag and lift coefficients are reproduced to verify cell

boundary element method. An, Cheng and Zhao (2015) simulated a cylinder in oscillatory flow with both two- and three-dimensional finite element models at *Re*=2000 and *KC*=1, 2, 5, 10, 17.5, 20 and 26.2. They showed that the 2D model is able to capture the majority of the genuine flow structures and hydrodynamics loads when compared to 3D models.

On the contrary, research on the multiple cylinders or even simply two cylinders in the oscillatory flow is much rare and far more complex compared to the single cylinder case, as the additional cylinder will introduce hydrodynamic interference between cylinders which will alter the hydrodynamic performance significantly. Williamson (1985) found in his experiments of two cylinders with varying gaps oscillating in the still water at different *KC* number that the vortex shedding from the two cylinders may achieve synchronization in either phase or anti-phase depending on the *KC* number. And some numerical work has been performed, as Zhao and Cheng (2014) carried out a 2D simulation for dual cylinders with varying gaps in both side-by-side and tandem configuration, and he classified and presented a variety of flow regimes (such as new GVS regime of gap vortex shedding) for the dual cylinders depending on *KC* and β range.

In this study, we performed both an extensive experimental study for two cylinders oscillating in the still flow with a side-by-side configuration and a detailed 2D numerical simulation visualizing the flow pattern around the dual cylinders. An emphasis on the drag enhancement phenomenon of the dual cylinders will be presented.

EXPERIMENTAL SETUP AND RESULTS: FORCE COEFFICIENCT MEASUREMENT

The experiments are conducted in the small tank at *MIT Tow Tank*, and the sketch of the setup is shown in Fig. 1. The experiment covers the range of Keulegan-Carpenter Number from 1 to 20 and the range of Strokes number from 350 to 2810. And the gap ratio (Gap/Diameter) is set as 0.5, 1.0, 2.0 and 3.0 for dual cylinder cases. And the cylinders are forced a prescribed sinusoidal oscillation in the still water. With the simultaneous force and motion measurement, the cylinder in-line force is able to be separated into added mass component C_m (in phase of acceleration) and drag force component C_d (in phase of velocity), in the Morison Equations, with a least square method. Experiments with each cases are repeated for at least three times on different days. And cylinders with various diameters are adopted to achieve a wide range of beta numbers, shown in Fig. 2. In the side-by-side cases, the experiment arrangement is shown in the Fig. 1. The tank is large enough to ensure the vortex will not reach the boundary in the experiment and hence free of wall effect. The same consideration is also adopted in the experiment of single cylinder cases as well as later numerical simulations.

The similar experiments of single circular cylinder in viscous oscillatory flow are also conducted by Sarpkaya at 1986 and Bearman at 1985 (static cylinder in the oscillatory flow condition). Our results are compared with the result of Sarpkaya and are shown in the Fig. 3. Although there are slightly difference between Strokes number of our experiments, the trend is almost the same. With KC number increasing, the C_m coefficients are all decreasing and C_d coefficients are mainly enhanced, although a period of flatness of C_d appears in Sarpkaya's result and this may correspond to vortex shedding pattern transition, which hasn't appeared in our result.

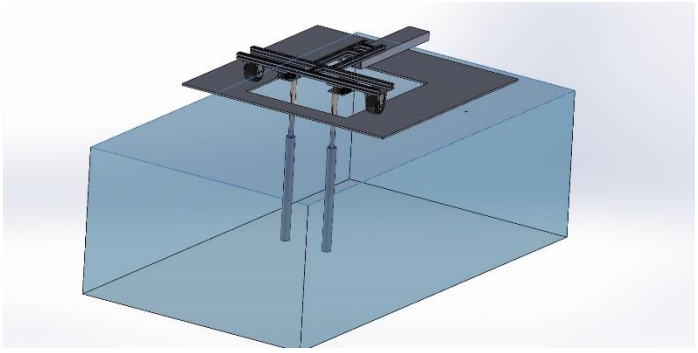

Fig. 1 Small tank at MIT Tow Tank

Fig. 2 Experimental models

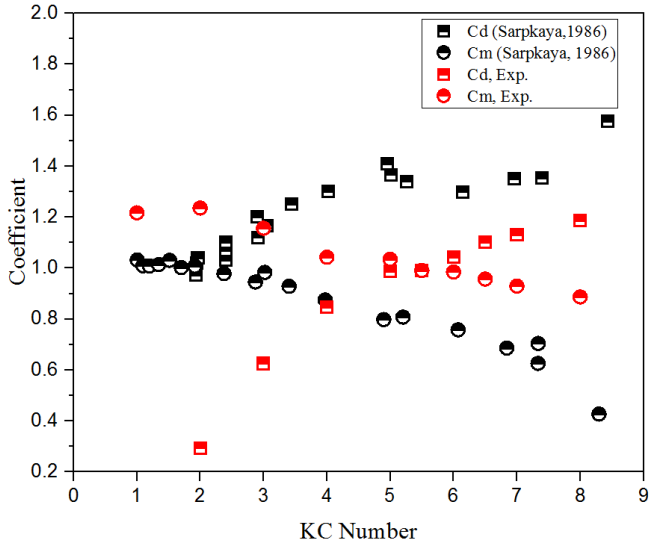

Fig. 3 Comparison of results (Exp.: β=1400; Sarpkaya: $\beta = 1380.$)

As for dual cylinders in oscillatory flow, the flow field is much messier when compared with single cylinder cases due to the generation of a much stronger wake because of the dual cylinder interaction. When dual cylinders undergoes sinusoidal oscillation, the in-line force coefficient and the corresponding cylinders' trajectory are shown together in both Fig. 4 and Fig. 5 for different cases respectively. We can see that depending on the KC and beta number, the amplitude of the coefficient and its phase angle towards the motion will be different.

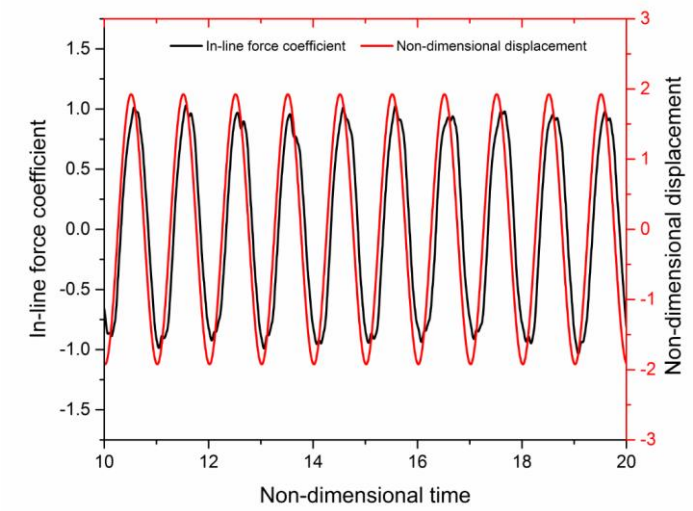

Fig. 4 Non-dimensional displacement and in-line force vs time (Side-by-Side, KC =12.1, $\beta = 480$, Gap Ratio=0.5)

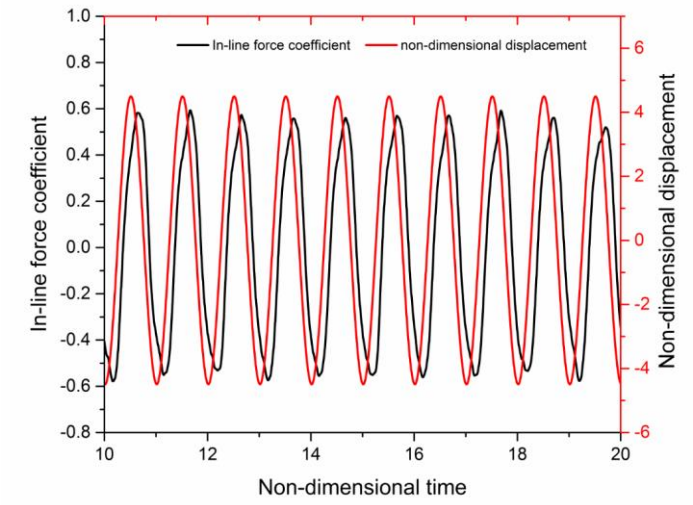

Fig. 5 Non-dimensional displacement and in-line force vs time (Side-by-Side, KC =28.2, $\beta = 480$, Gap Ratio=0.5)

The in-line force and position of one cylinder are with the same frequency in these cases and are almost in the same phase, but the phase of position is a little ahead than that of in-line force as the wake and vortex in the flow field has inertia and it needs a little time for flow field to adjust and further influence the in-line force. The positions in the results are both standard sinusoidal motion to verify the experimental accuracy. However the in-line force is not standard sinusoidal oscillation as it is the sum of added mass force and drag force. Moreover, when KC is larger, the in-line force amplitude in each period is not steady, which agrees with Ming Zhao (2014)'s result that when KC is large, the result and flow field tend to be irregular.

The in-line force is further separated into drag force and added mass force coefficients. We choose the cases with β of 1190, and the result of C_d and C_m vs different KC numbers for various gap ratios are shown in the Fig. 6 and Fig. 7 respectively.

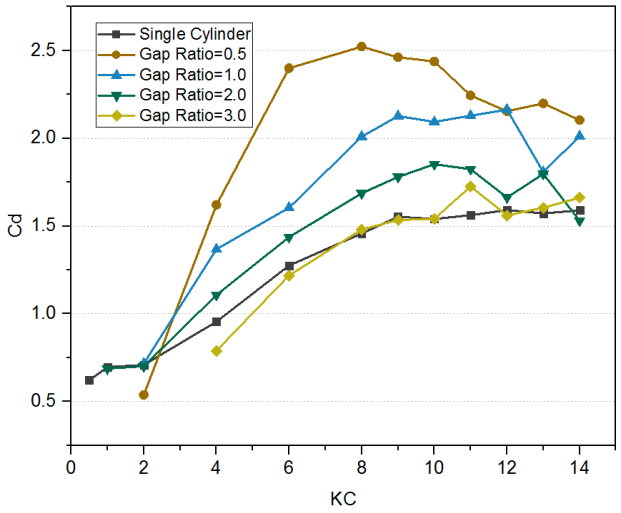

Fig. 6 Drag Coefficient vs KC ($\beta = 1190$)

When gap ratio is large as 3, the drag coefficient has the same trend and almost same as the single cylinder, because the interaction between cylinders is weak for the large gap. And, strikingly, drag coefficient tends to increase with the decrease of the cylinder gap for a wide range of the KC number and hence the drag enhancement is identified for the small cylinder gap when cylinder interaction is stronger. The same trend is also found in the added mass coefficient that when gap ratio equals to 3, the added mass is quite similar to that of single cylinder. And we can also observe that added mass coefficient with gap ratio of 0.5 is greatly enhanced when KC is larger than 6. However, the enhancement of added mass coefficient is not appeared in cases of all other β numbers and the reason of such enhancement will be investigated in the near future.

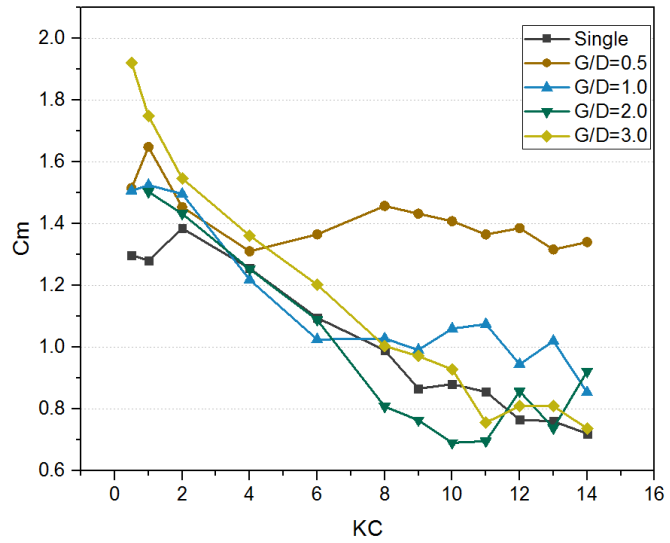

Fig. 7 Added Mass Coefficient vs KC ($\beta = 1190$)

In order to better reveal the drag coefficient enhancement, we plot the enhancement factor, which is defined as the drag coefficient Cd of the dual cylinder over that of the single cylinder for the same KC and beta number. Fig. 8 shows the enhancement factor for different beta number under KC = 6, and therefore area above the black horizontal line equaling to 1 indicates an enhanced drag coefficient compared to that

of the single cylinder. We can see that at KC = 6, for all the beta range in the current experiment the drag coefficients are amplified for the case of gap ratio of 0.5 and 1.0.

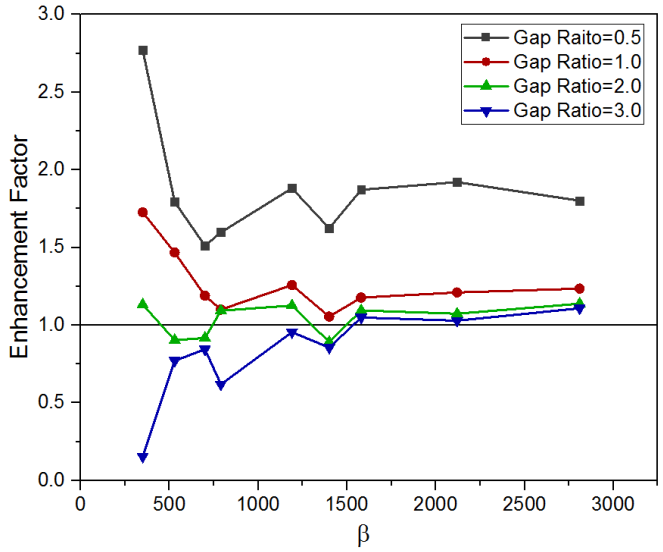

Fig. 8 Enhancement factor vs β number for KC=6.

NUMERICAL SIMULATIONS: FLOW PATTERN ANALYSIS

As described in the last section of the experiment of the dual cylinder oscillating in the still water, we found that when gap ratios decrease, namely two cylinders are closer, the drag coefficient enhancement is much stronger. This indicates that there must be some strong wake interaction of two cylinders that results in a stronger energy dissipation from the structure to fluid, as in the Morison Equation, the drag force is the dissipative term while added mass force is the conservative term, which can be revealed through the following two integrals if we assume that $U(t) = Asin(\omega t)$:

$$\int_0^T \frac{1}{4}\pi\rho D^2 C_m \frac{dU(t)}{dt} \cdot Udt = 0 \tag{2}$$

$$\int_0^T \frac{1}{2}\rho D C_d |U(t)|\, U(t) \cdot U(t)dt = \frac{4}{3\omega}\rho D C_d A^3 \tag{3}$$

In order to get more detailed flow field information related to this phenomenon, further numerical simulation is conducted with the feasibility and computability of flow field information that helps to shed some light on this phenomenon.

The solver used in this paper is Lily-Pad based on BDIM developed by Weymouth and Yue (2011) to solve the problems of immersion of solid bodies within a fluid with general boundary conditions. BDIM is based on a general integration kernel formulation which combines the field equations of each domain and the interfacial conditions analytically. The resulting governing equation for the complete domain preserves the behavior of the original system in an efficient Cartesian-grid method, including stable and accurate pressure values on the solid boundary.

The numerical simulation arrangement is shown in the Fig. 9, and it is quite similar to experimental arrangement, except that the simulation is in 2-dimension and an energy outflow calculation control volume is added into the calculation domain. The control volume can help us pick and record the velocity and pressure information on the boundary of this volume. The volume is with length of 4D and width of 8D to satisfy the demand of large motion amplitude. The tank boundary is impenetrable, thus the size of the calculation domain is $40D \times 20D$ to erase the boundary effect and block effect, which is quite influential in this study. The solver of Lily-Pad does not need us to establish meshes, and the pixel of the screen will directly be the nodes of mesh to establish unstructured meshes. However, we have to define the size of cylinders and domains with unit of pixel. In this study, to balance the calculation efficiency and accuracy, the diameter of each cylinder is set to become 50 pixels.

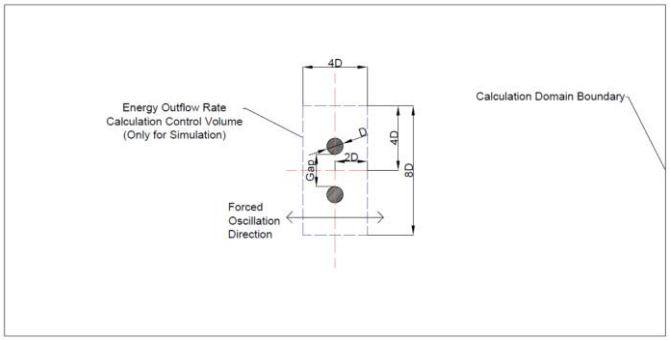

Fig. 9 numerical simulation arrangement

Before the calculation of dual cylinders, a mesh dependent study has been conducted with single cylinder cases for code verification. The diameter to mesh ratio we use in validation cases are 37.5, 50 and 62.5. KC of 7 and Reynolds number of 120 is picked for all three cases. The calculated added mass coefficient and drag coefficient are listed in the Table 1.

Table1. Mesh dependent study for single cylinder (KC=7, Re=120)

Diameter to mesh ratio	C_m	C_d
37.5	1.8850	2.4578
50	1.9335	2.3768
62.5	1.9461	2.3507

The relative error for C_m decreases from 2.57% to 0.65% when diameter to mesh ratio increases from 37.5 to 50 and further to 62.5. The relative error for C_d also decreases from 3.30% to 1.10% in the same comparison. In Fig. 10, we can also find that the vorticity field at non-dimensional time of 65 with diameter to mesh ratio of 50 and 62.5 is almost the same. The details in Fig 10(c), such as the shake of negative vorticity contour outline, can also be clearly observed in Fig 10(b). However, the result with diameter 37.5 in Fig 10(a) is different and the phenomenon of asymmetry, which also appear in the flow visualization result of Tatsuno and Bearman (1990) starting from regime D, does not develop fully. Thus the final selected mesh with the diameter to mesh ratio of 50 can satisfy the demand of accuracy. In this setting, the total mesh cell number will become about 2 million. However, the simulation is very fast in practical using, which is mainly due to the algorithm of BDIM.

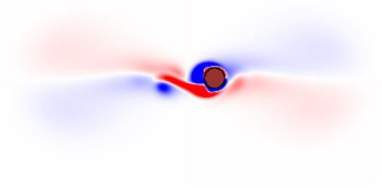

(a) Diameter = 37.5

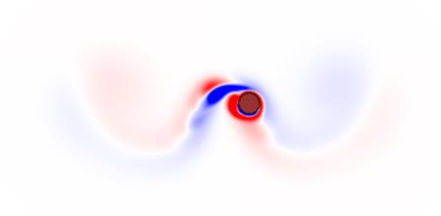

(b) Diameter = 50

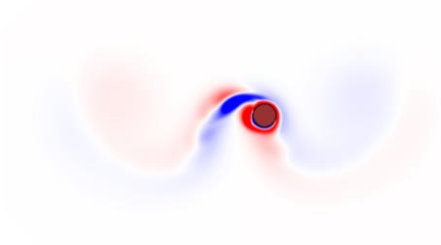

(c) Diameter = 62.5

Fig. 10 Comparison of vorticity field at time of 65 with different meshes at KC =7

Furthermore, all the parameters in simulation are non-dimensionalized as $(x, y) = (x', y')/D$, $(u, v) = (u', v')/U_m$, $p = p'/\rho U_m^2$, and $t = U_m t'/D$. Where (x, y) are the point in Cartesian coordinates, (u, v) are the velocity component in x and y direction respectively, t is time, p is pressure, ρ is the density of the fluids, U_m is the maximum velocity of the cylinder's forced motion. In the simulation, the Reynolds number of all the cases are set to be a fixed value of 120 and KC numbers are 6 and 7. Strokes numbers vary according to Reynolds number and KC numbers as $\beta = Re/KC$. Within dual cylinder cases, the gap ratios are 0.50, 0.60, 0.70, 0.75, 0.90, 1.00, 1.25, 1.50, 1.60, 1.75, 2.00 and 3.00.

In the 2-D numerical simulations, the phenomenon of drag coefficient enhancement is also observed and the result of drag coefficient is shown in the following Fig. 11 for KC of 6 and Fig. 12 for KC of 7.

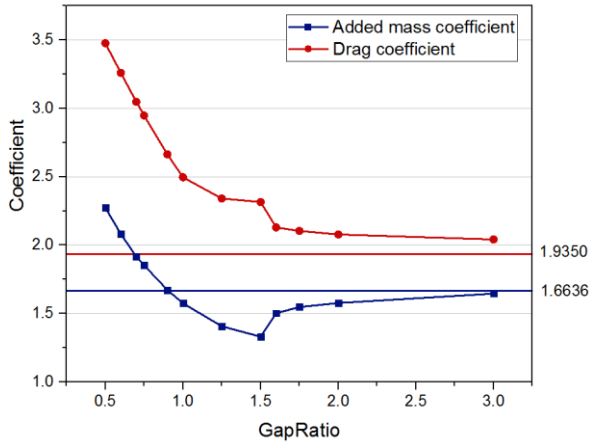

Fig. 11 Result of force coefficient at KC of 6

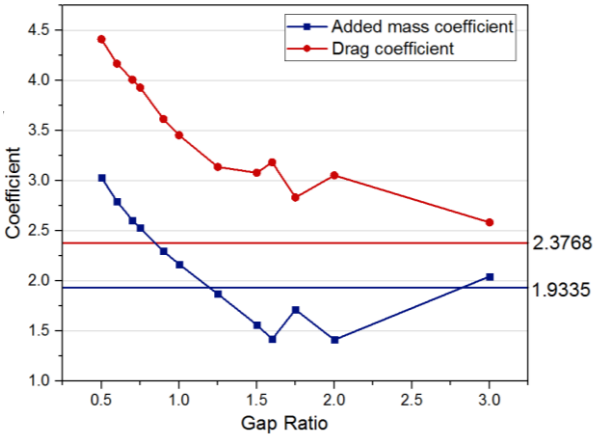

Fig. 12 Result of force coefficient at KC of 7

In Fig. 11 and Fig. 12, the horizontal lines in red and blue are the drag coefficient and the added mass coefficient of single cylinder. In these two figures, C_d and C_m are both decreasing firstly with increasing of gap ratio, and then when the gap ratio reaches nearly 1.50, and then slowly converges to the single cylinder coefficient value. This is expected as when the gap ratio is large enough, the interaction of wake of two cylinders is very weak, and hence two cylinders can barely "feel" each other. These phenomena are also revealed by experiment, and therefore the numerical, in general, well captured the major physics of the experiment.

The vorticity contour of single cylinder with KC at 6 is shown in the Fig. 13. When the cylinder moves to the furthest left end, the vortex A in Fig. 13(a) shed in last half cycle is moving into the right region where vorticity is decaying. While at that time point, an opposite pair of vortices B in Fig. 13(a) starts to form near the cylinder, and will be soon developing quickly in Fig 13(b). At the same time, the main wake vortex C in last half period quickly sheds, gradually moves into the left vortex region and becomes weaker and weaker in this progress. The main wake vortex in this half period B attach to the cylinder, and does not detach during the motion in this half period. And then main vortex in next half period D forms near the cylinder as shown in Fig 13(d). When this half period ends, next half period begins and the vortex shedding is just like a circulation. The vortex B will shed in next half period. In this pattern, we can see that the wake shed into the background is so weak and it is not expelled far away even if the time is quite long.

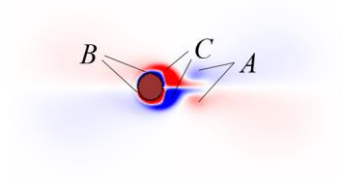

(a) Time of 63

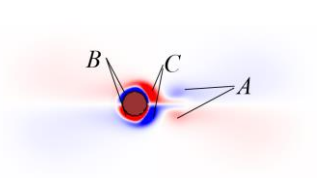

(b) Time of 63.36

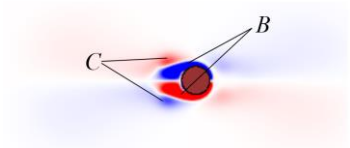

(c) Time of 64.17

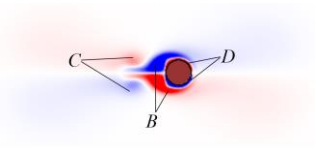

(d) Time of 64.95

Fig. 13 The vorticity contour in a half period (KC=6)

But the vortex in the case of dual cylinder with small gap ratio exhibits a different behavior. The vortex wake of the dual cylinder with a gap ratio of 0.5 in a half period is shown in the Fig. 14. The Fig. 14(a) is the furthest left position. In Fig. 14(a), the wake at first is quite similar to that of single cylinder that wake B and C with opposite vortex are going to form on the upper and lower cylinder separately. But this time, wake of each cylinder B and C is not symmetrical, and it inclines to the central line. Moreover, in Fig 14(b) the lower vortex of upper cylinder and upper vortex of lower cylinder interact strongly and become a vortex pair D and the outer vortex of each cylinder becomes E and F. This vortex pair D forms a strong jet in the gap and hence induces a large initial velocity that helps themselves to leave away from the cylinders more quickly. When the cylinders move to the right largest displacement in Fig. 14(d), the main vortex pair D is going to shed. At this time, the cylinders have stopped moving, but the main vortex pair D still has a large velocity to left. Then the cylinders move leftward in Fig. 14(e), the main vortex pair D left the cylinder, and a small vortex pair D_2 forms, which combines the clockwise vortex from the upper cylinder and anticlockwise vortex from lower cylinder. The vortex shed into main vortex pair D_1 is not all the vortex, and the vortex D_2 near the cylinder still moves with the cylinder in Fig 14(e) and it is quickly neutralized by strong vortex G in the next half cycle in Fig 14(f). And then E and F shed and become weaker due to the influence of H and I, just like vortex A in the last half period.

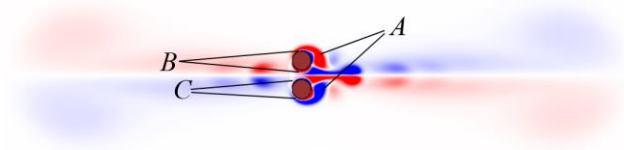

(a) Time of 62.93

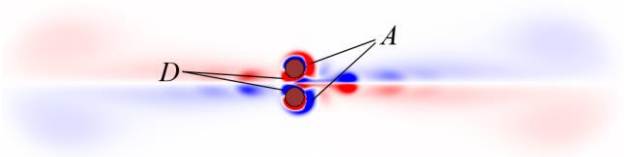

(b) Time of 63.33

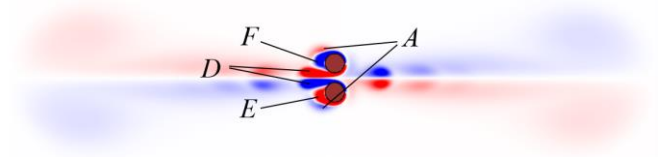

(c) Time of 64.07

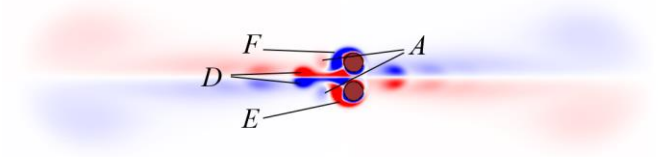

(d) Time of 65.00

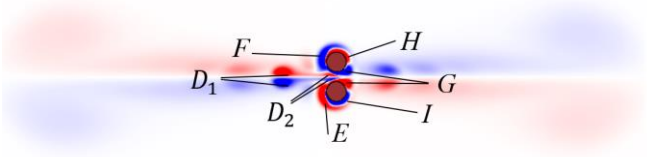

(e) Time of 65.42

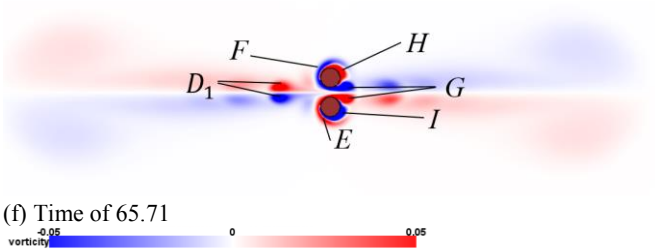

(f) Time of 65.71

Fig.14 Vorticity development for dual cylinders (KC=6, Gap ratio=0.5)

Tracking the vortex pair left the cylinder, we can see that the vortex pair are able to maintain its shape and also achieve high velocity away from the cylinder for a much longer time and distance, compared to the faster decayed vortex wake in the single cylinder case. And therefore, the vortex pair generated between the gap is one of the key factors to help an energy transfer / dissipation from the cylinder to the fluid into the far flow field, Thus this explains that phenomenon of the enhancement of drag coefficient which is directly associated with the energy transfer between the fluid and structure.

In order to further verify this, we performed an energy outflow rate calculation through the integral of the kinetic energy about the control volume that includes the dual cylinders region at every time point. This allows us to monitor the amount of the kinetic energy across the boundary that carried in the vortex wake. The time series of EOR (Non-dimensional Energy Outflow Rate) in the cases with gap ratio of 0.5, 1.0, 2.0, 3.0 and single are therefore shown in Fig. 15. In this paper, Non-dimensional Energy Outflow Rate are defined and calculated as the following Eq. 4 shows, and will be simplified as EOR:

$$EOR = \oint \frac{1}{2} |\vec{u}|^2 \vec{u} \cdot \vec{n} \, ds \tag{4}$$

Where $\vec{u}$ is the non-dimensional fluid particle velocity at the node on the boundary of control volume, $\vec{n}$ is the outward normal vector of control volume boundary, while *ds* is the non-dimensional length of line segment between neighbor nodes along the boundary of control volume.

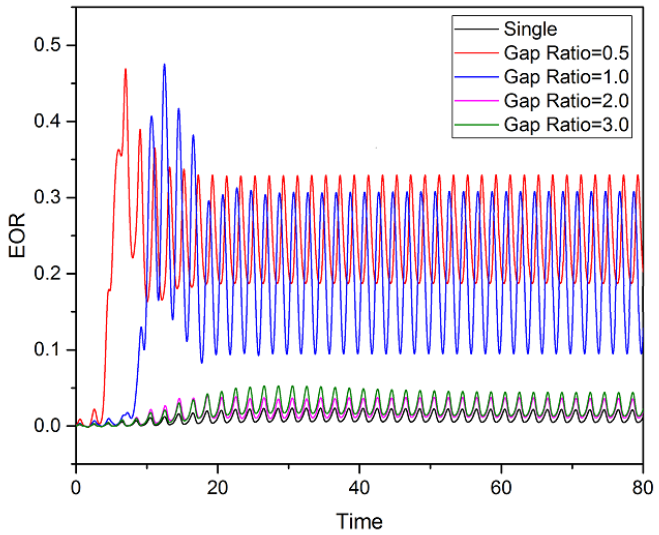

Fig. 15 EOR in some specific cases (KC=6)

In the Fig. 15, we saw that EOR begins to jump from 0 and fluctuate

firstly for the dual cylinder with gap ratio of 0.5, compared to the others. This indicates a vortex pair with a larger initial velocity and hence it is able to reach the boundary of control volume more swiftly.

After a further calculation of the mean EOR for each cylinder, defined as *mean EOR of one period / Number of cylinders*, the results are plotted in Fig. 16. In Fig. 16, the trend of energy outflow rate agrees well with drag coefficient, although it shows an increase in the first beginning. This may relate to the growth of the volume of the vortex pair due to the larger gap.

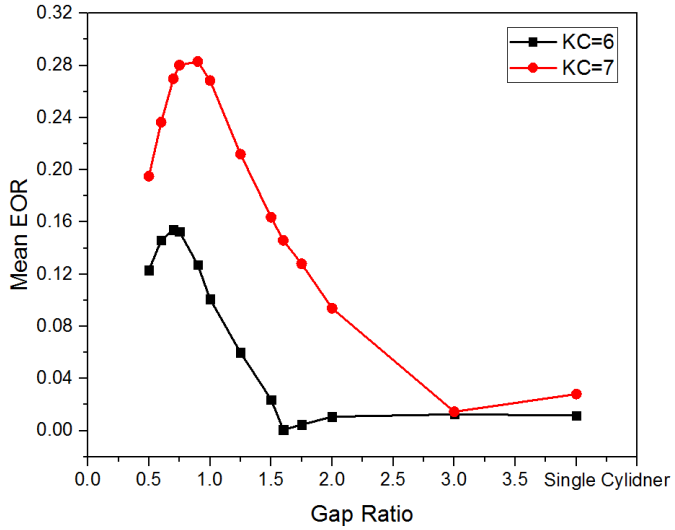

Fig.16 Mean energy outflow rate

When the gap ratio is going to increase from 0.5, the vortex pair is still obvious when gap ratios are small, although some slight difference may appear in the development of this phenomenon. The vorticity field of cases with different gap ratios at time 66 is shown in Fig. 17. In Fig. 17(a) for gap ratio of 0.6, we can see that a small additional vortex pair with opposite direction forms during the whole progress due to the larger gap and the interaction is slighter compared with gap ratio of 0.5. With gap ratio continuing to increase, the interaction further weakens and the velocity of the vortex pair is going to decrease. When the gap ratio gets to 1.25, the symmetrical vortex pair disappears, but the vortex pair still exists thus the drag coefficient is still larger than single cylinder case. The vortex wake with gap ratio of 1.75 and 2.00 are almost the same and the directions that vortex moves have a large angle to the central line. When the gap ratio is 3, the interaction is relatively weak, thus the wake is quite similar to the case of single cylinder.

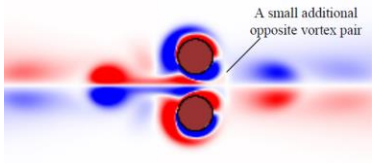

(a) Gap ratio =0.6 at time of 65.32

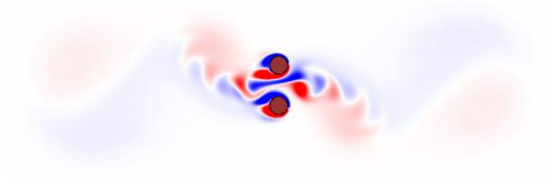

(b) Gap ratio of 1.25 at time of 66.01

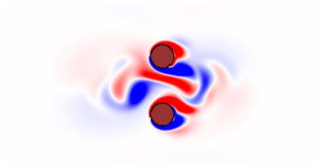

(c) Gap ratio of 1.50 at time of 66.02

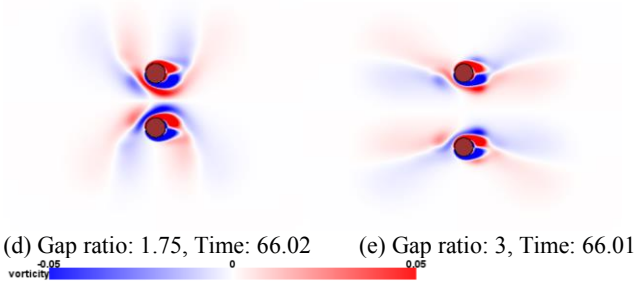

(d) Gap ratio: 1.75, Time: 66.02 (e) Gap ratio: 3, Time: 66.01

Fig. 17 vorticity contour of larger-gap cases

In the cases with small gap ratio, the gap vortex jet can be clearly observed and the drag coefficient is much larger than the cases in the flow regime without this jet. When the jet disappears, the enhancement is also greatly weakened. Thus it is reasonable to attribute the enhancement of drag coefficient to gap vortex jet.

CONCLUSIONS

In this paper, we focused on the hydrodynamic problems of the dual cylinders in the oscillatory flow with a side-by-side configuration. First the phenomenon of drag enhancement is found universal in the experiment for the dual cylinders at small gap ratio, compared to the single cylinder in the oscillatory flow. Numerical simulation at a smaller Reynolds number of 120 and KC of 6 and 7 confirms the phenomenon and a strong jet of a vortex pair forming between the center gap is observed with the wake visualization. This jet takes large kinetic energy from the cylinder and quickly dispels it into far flow field, and this is quantified by the calculation of mean energy outflow rate (EOR). And Therefore we conclude that the gap vortex jet due to strong interaction of two cylinders wake is one of the major factors that cause the enhancement of drag coefficient.

ACKNOWLEDGEMENTS

The support of Dr. G.D. Weymouth, who established and provided the solver of Lily-Pad used in this paper, is gratefully acknowledged.

REFERENCES

An, H., Cheng, L., & Zhao, M. (2015). Two-dimensional and three-dimensional simulations of oscillatory flow around a circular cylinder. *Ocean Engineering*, 109, 270-286.

Bearman, P. W., Graham, J. M. R., Downie, M. J., & Obasaju, E. D. (1985). Forces on cylinders in viscous oscillatory flow at low Keulegan-Carpenter numbers. *Journal of Fluid Mechanics*, 154(337-356), 14.

Fan, D. Hydrodynamic performance of multi-component structures in oscillatory flow, from blow-out preventer to dual cylinder interference. *Diss. Massachusetts Institute of Technology*, 2016.

Morison, J. R., Johnson, J. W., & Schaaf, S. A. (1950). The force exerted by surface waves on piles. Journal of Petroleum Technology, 2(05), 149-154.

Sarpkaya, T. (1986). Force on a circular cylinder in viscous oscillatory

flow at low Keulegan—Carpenter numbers. *Journal of Fluid Mechanics*, 165, 61-71.

Tatsuno, M., & Bearman, P. W. (1990). A visual study of the flow around an oscillating circular cylinder at low Keulegan–Carpenter numbers and low Stokes numbers. *Journal of Fluid Mechanics*, 211, 157-182.

Uzunoğlu, B., Tan, M., & Price, W. G. (2001). Low‐Reynolds‐number flow around an oscillating circular cylinder using a cell viscousboundary element method. *International Journal for Numerical Methods in Engineering*, 50(10), 2317-2338.

Weymouth, G. D., & Yue, D. K. (2011). Boundary data immersion method for Cartesian-grid simulations of fluid-body interaction problems. *Journal of Computational Physics*, 230(16), 6233-6247.

Williamson, C. H. K. (1985). Sinusoidal flow relative to circular cylinders. *Journal of Fluid Mechanics*, 155, 141-174.

Xu, Y., Fu, S., Chen, Y., Zhong, Q., & Fan, D. (2013). Experimental investigation on vortex induced forces of oscillating cylinder at high Reynolds number. *Ocean Systems Engineering*, 3(3), 167-180.

Zhao, M., & Cheng, L. (2014). Two-dimensional numerical study of vortex shedding regimes of oscillatory flow past two circular cylinders in side-by-side and tandem arrangements at low Reynolds numbers. *Journal of Fluid Mechanics*, 751, 1-37.